

INSTITUTE
OF ECONOMICS



Scuola Superiore
Sant'Anna

LEM | Laboratory of Economics and Management

Institute of Economics
Scuola Superiore Sant'Anna

Piazza Martiri della Libertà, 33 - 56127 Pisa, Italy
ph. +39 050 88.33.43
institute.economics@sssup.it

LEM

WORKING PAPER SERIES

The arrival of the new

Luigi Marengo ^a
Paolo Zeppini ^{a,b,c}

^a Institute of Economics, Scuola Superiore Sant'Anna, Pisa, Italy

^b School of Innovation Sciences, Eindhoven University of Technology,
Eindhoven, The Netherlands

^c CeNDEF, University of Amsterdam, The Netherlands

2014/04

February 2014

ISSN (online) 2284-0400

The arrival of the new

Luigi Marengo^a and Paolo Zeppini^{a,b,c}

^a *Laboratorio di Economia e Management, Scuola Superiore Sant'Anna, Pisa*

^b *School of Innovation Sciences, Eindhoven University of Technology*

^c *CeNDEF, Faculty of Economics and Business, University of Amsterdam*

Abstract

In this work we present a number of urn models in which, contrary to standard Pólya urns, the number of competing alternatives is not given from the outset but may increase with the arrival of innovations. We begin by describing a variant of Pólya urns, first introduced by Fred Hoppe, in which balls of previously non existing colours are added with some (declining) probability. We then propose new variants in which the probability of the arrival on new colours is itself subject to adaptive change depending on the success of past innovations. We numerically simulate different specifications of these urns with adaptively changing mutation rate and show that they can account for complex patterns of evolution in which periods of exploration with clusters of innovations are followed by periods in which the dynamics of the system is driven by selection among a stable set of alternatives.

1 Introduction

One of the most challenging questions in social sciences is how an innovation (an innovative technology, a new business model, a new behaviour or norm, etc.) can lead to a major transition in society. Models of path-dependence and lock-in have been successful in explaining the probabilistic laws governing the competing adoption process when a given set of options are available. Such models are based on the so-called Pólya-urn schemes, special types of Markov chains where the probability distribution of outcomes depends on past draws. They have been very successful in providing valuable insight in the study of path dependency in technological diffusion (Arthur, 1989; Arthur et al., 1987; Dosi et al., 1994), of reinforcement learning in signalling games (Erev and Roth, 1998), and in other economic models. However, these models are “closed world” models which only analyze the stochastic processes of selection among a given set of options, for instance two or more competing technologies. The implicit assumption is that the competing technologies come to existence at the same time and are not going to be challenged by further innovations. Pólya-urn models are instead agnostic regarding the origin of such options and fail to address the interplay between the complex interaction between the processes of selection (adoption) and innovation.

An extension of Pólya-urn models has been proposed in theoretical biology by Hoppe (1984) as a benchmark model for neutral drift in evolution, where mutations do not carry any selective advantage. Hoppe-Pólya urns extend the standard Pólya-urns model by adding a stochastic

process of addition of new options which before did not exist and enter the competition for selection. Thus, potentially, Hoppe-Pólya urns can account for genuine innovation and persistence of variety. However, we will show, also in this model the rate of innovations approaches zero rather quickly, and an initial phase of exploration is followed by endless exploitation. In this article we propose a variant of Hoppe-Pólya urn models consisting in an adaptive rate of mutation. The rate of arrival of new options is itself subject to a self-reinforcing mechanism: if innovations are successful the rate of innovation tends to increase, whereas if the new options recently introduced perform worse than the incumbent options, also the rate at which new options are introduced tends to fall.

The model is as follows. Different alternative options are represented as coloured balls in a urn. One ball is drawn at random. Self-reinforcement is accounted for by adding a ball of the same colour after each draw. This is the classic Pólya-urn model. Mutation is introduced in Hoppe-Pólya urns with a black ball. If the black ball is drawn, a new colour, which did not exist before, is added to the urn. In our model the black ball, the mutator, has an adaptively changing mass: successful innovations do not only add a new colour to the urn, but also increase the mass of the black ball, so that it will be more likely drawn.

In this paper we provide a detailed study of the numerical properties of our variant of Hoppe-Pólya urn model with adaptive mutation rates. The distribution of simulation outcomes shows more variety than a simple Hoppe-Pólya model, with sustained novelty and different phases in the interplay between innovation and selection. The time evolution of the process shows that variety is not constant, but displays a pattern of punctuated equilibrium. Thanks to the endogenous rate of mutation, successful innovations establish themselves, but after some time newer successful innovations come about and take over the incumbents. The intuition is that while self-reinforcement of each option is marginally decreasing, the reinforcement mechanisms of the mutator is not, so, in the long run, the process of novelty is sustained, while incumbent options have an intrinsic weakness stemming from their old success.

The time required for a transition to occur is function of the competition process between alternative innovations. Once “winning” innovation has emerged from this competition, the incumbent’s decline begins (*“sic transit gloria mundi”*). The pattern of variety produced by our model may describe conceptually technological transitions. One example is the energy sector, where a number of alternative renewable energy solutions (Solar, Wind, Biomass, Fuel-cells) compete among themselves to be the right alternative to fossil fuels. In a broader sense, our model can be relevant to more general societal transitions, proposing a probabilistic explanation of the rise and fall of organizations and societies.

To our knowledge, the only existing application of Hoppe-Pólya to a socio-economic problem is contained in Alexander et al. (2012). They use Hoppe-Pólya urns to analyze a signalling game (Crawford and Sobel, 1982) with reinforcement learning *à la* Erev and Roth (1998). They introduce the possibility that new signals can be stochastically introduced, which in this context becomes a way to escape pooling equilibria and increase the probability of convergence to separating equilibria. Once equipped with a reinforcement learning mechanism, Hoppe-Pólya urns are not neutral anymore, and display selective advantage instead. Contrary to them, our selective advantage operates not on the coloured balls, but directly on the black one, therefore modifying the rate of mutation. This prevents early lock-in of the system in a limited set of options¹ and can produce sustained innovation.

The paper is organized as follows. In section 2 we briefly describe Hoppe-Pólya urn models and our variant with adaptive mutation rates. In section 3 we present, as benchmark cases, numerical results from the simulation of both standard Hoppe-Pólya urns and urns with non-adaptively increasing mutation rates, while in sections 4 and 5 we describe the behaviour of our adaptive version when fitness values are drawn, respectively, from a uniform distribution and

¹Alexander et al. (2012) model a very simple signalling game with a very small set of strategies and signals. If they had a larger set of options their results would not necessarily hold.

from a Beta distribution. In section 6 we use fitness values not only to modify the probability of the introduction of new colours but also the probability of addition of balls of the existing colours. Finally, in section 7 we summarize and conclude.

2 The model

2.1 Hoppe-Pólya urns

Proposed by Fred Hoppe in Journal of Mathematical Biology in 1984 as a benchmark model for neutrality in evolution, Hoppe-Pólya urns model neutral selection, especially in those case in which there exist a vast number of potential mutations which convey no selective advantage, and extend Bayesian theory of induction, generalizing the Bayes-Laplace rules of succession allowing for the formation of new categories (Zabell, 1992).

A Hoppe-Pólya urn at time 0 contains only one black (“uncoloured”) ball and at time n it contains 1 black ball and n coloured balls of k different colours. At each time $n + 1$ one ball is randomly drawn from the urn. If a coloured ball is drawn it is reintroduced in the urn together with a new ball of the same colour (as in a standard Pólya urn), thus at time $n + 1$ we have $n + 1$ coloured balls of k different colours (we remind once more that the black ball is not counted among the coloured ones). If instead the black ball is drawn, it is reintroduced in the urn together with a new ball of a **new colour**, thus at time $n + 1$ we have $n + 1$ coloured balls of $k + 1$ different colours. As an extension we can suppose that the black ball has mass $\theta > 0$, whereas coloured balls have all mass 1.

Obviously, in the urn process we just described the number of colours grows logarithmically to infinity, as the expected number of colours at time n is given by the harmonic series $\sum_{i=0}^n 1/i$. Figure 1 plots the expected number of colours in the logarithm of time.

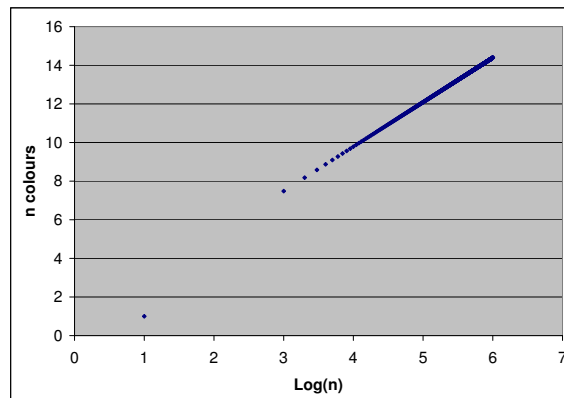


Figure 1: Expected number of distinct colours

A Hoppe-Pólya stochastic process can be formalized as follows. Let us call $\{1, 2, \dots\}$ the set of colours (once more, black is not consider a colour, it is a mere “mutator”) and X_n the random variable which indicates the colour of the new ball added to the urn after the n -th drawing. If we start with only one black ball in the urn we have $X_1 = 1$, $X_2 = 1$ or 2 , $X_3 = 1, 2$ or 3 , etc..

Let k be the random number of distinct colours that are in the urn at time n , then the urn can be described as a set of k integers $\{n_1, n_2, \dots, n_k\}$ which form a partition² of the integer n . Which one among the possible partitions of n will be realized depends upon the sequence $\{X_j\}_{j=1}^n$ of draws.

²A partition of a positive integer n is a way of writing n as a sum of positive integers. For instance, the integer 4 can be partitioned in five ways: 4, 3+1, 2+2, 2+1+1, and 1+1+1+1.

For each $1 \leq i \leq n$, call a_i the number of times the integer i appears in $\{n_1, n_2, \dots, n_k\}$, the vector $a = (a_1, a_2, \dots, a_n)$ is called the (allelic) partition vector. For instance, $a = (1, 0, 1, 0)$ indicates that there is one colour with three balls and one colour with one ball (thus $n = 4$).

For a given number of colours, the distribution of trials among the possible partitions is not uniform. Suppose, for instance, we have two colours after 10 trials (this happens with probability $\simeq 0.28$). This can be realized in 5 different ways as a partition of 10: 5+5, 4+6, 3+7, 2+8, 1+9. As we will show below, the probability of each partition is given by Ewens' sampling formula (Ewens, 1972):

$$P[a_1, \dots, a_n] = \prod_{j=1}^n \frac{1}{j^{a_j} a_j!}$$

As an example, Figure 2 plots the probabilities of each such partitions for the case of 10 trials and 2 colours. It can be noticed that more “unequal” partitions are more likely. This property is called *preferential attachment*, meaning that more crowded cells are more likely to attract new tokens, and obviously reflects the property of increasing returns of the urn process.

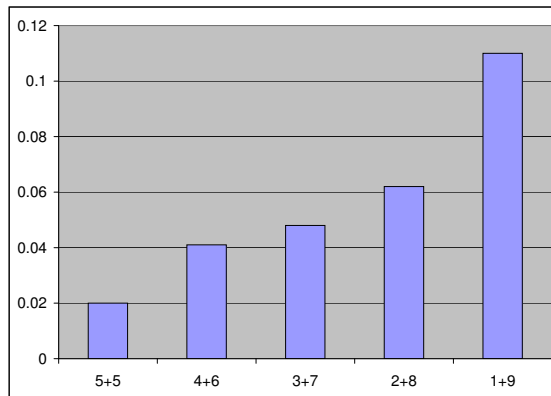


Figure 2: Probabilities of partitions of 10 trials into 2 colours

Assuming that the initial mass of the black ball is θ , the fundamental result in Hoppe-Pólya urns is the following:

Hoppe's Theorem: the random partition Π_n determined by the sequence $\{X_j\}_{j=1}^n$ is a Markov process with marginal distribution:

$$P[\Pi_n = a] = \frac{n!}{[\theta]^n} \prod_{i=1}^n \frac{\theta^{a_i}}{i^{a_i} a_i!} \quad (1)$$

where $[\theta]^n = \theta(\theta + 1) \dots (\theta + n - 1)$.

Hoppe (1984) provides a proof which uses combinatorial arguments³. Here we briefly summarize it.

Consider a partition $a = (a_1, a_2, \dots, a_n)$ with k distinct colours and a sequence of draws $\{X_j\}_{j=1}^n$ generating it. This sequence can be obtained with probability:

³Hoppe-Pólya urn processes are strictly connected to a family of combinatorial problems know as *occupancy problems*, and in particular to the so-called *Chinese restaurant problem* (see, e.g., Pitman, 2006), i.e. a restaurant with an infinite number of tables of infinite capacity. A *phantom guest* (the equivalent of the black ball in our urn) always sits at an otherwise unoccupied table, while regular customers enter the restaurant one at a time and sit at an already occupied table choosing them with probabilities proportional to the number of occupants already seated (phantom guest included).

$$P[X_1 = x_1, \dots, X_n = x_n] = \frac{\theta^k \prod_{j=1}^k (n_j - 1)!}{[\theta]^n} \quad (2)$$

The explanation is simple: in order to get k colours the black ball must be drawn k times and this happens with probability $\theta^k/[\theta]^n$, where the denominator is the product of the successive number of balls in the urn ($\theta, \theta + 1, \theta + 2$, etc.). Then in order to get exactly the required partition, each colour must be drawn exactly $n_j - 1$ times.

Now we have to count the number of sequences of draws which generate the required partition. Given a permutation, a cycle is a subset of its elements that trade places with one another and the number of elements of the subset is called the length of the cycle. For instance, in the permutation 4,2,1,3, (1,4,3) is a 3-cycle and (2) is a 1-cycle, meaning that starting from 1,2,3,4 we can obtain the above permutation by performing the following replacements: $1 \rightarrow 4 \rightarrow 3 \rightarrow 1$ and $2 \rightarrow 2$. It can be shown that every permutation can be expressed as a product of disjoint cycles (for instance $3,2,1,5,4 = (1,3)(4,5)(2)$; $2,5,4,3,1 = (1,2,5)(3,4)$, etc.).

Let $O = \{A_1, A_2, \dots, A_n\}$ be a set of objects and σ a permutation thereof. Express σ in its cycle decomposition and suppose it contains k cycles, labelled $\{1, 2, \dots, k\}$. Map each element in σ into its own cycle. For instance, the permutation $\sigma = (CEDABGF) = (ACD)(BE)(FG)$ with the mapping $(ACD) \rightarrow 1$, $(BE) \rightarrow 2$ and $(FG) \rightarrow 3$ can be written as (1211233). Note that there are $k!$ labellings but in only one of them the first appearance of 1 precedes the first appearance of 2, which precedes the first appearance of 3, and so on.

The mapping of permutations of n elements into strings of length n of the first k integers we just described is clearly many-to-one. Two permutations map into the same sequence of k integers if and only if their cycle representations contain the same groups of symbols. For instance the permutation $\sigma' = (DEACBGF) = (ADC)(BE)(FG)$ maps into the sequence (1211233), i.e. the same we previously found for σ . If a cycle contains n_j elements there are $(n_j - 1)!$ distinct cycles with the same elements, hence the mapping has multiplicity $\prod_{j=1}^k (n_j - 1)!$.

To each permutation σ there corresponds a partition $a = (a_1, a_2, \dots, a_n)$ of n defined by $a_i = a_i(\sigma)$, i.e. the number of cycles of length i in the representation of σ . The number of permutations whose cycle decomposition determines a given partition a is $n! / \prod_{i=1}^n i^{a_i} a_i!$. Hence the number of distinct paths is:

$$\frac{n!}{\prod_{i=1}^n i^{a_i} a_i! \prod_{j=1}^k (n_j - 1)!} \quad (3)$$

By multiplying 3 and 2 we finally obtain equation 1.

2.2 Urns with adaptive mutation rates

In Hoppe-Pólya urns the rate of mutation quickly vanishes as the probability of drawing the black ball at time n is $\theta/(\theta + n - 1)$. Thus we tend to observe early lock-in and the disappearance of any further exploration. This is especially unfortunate if the state space is large and/or non stationary.

We propose therefore a variation of Hoppe-Pólya urns where the mutation rate is itself subject to variability and adjusts in an adaptive fashion. First of all we have to depart from the assumption of neutrality and suppose that colours have differential adaptation to the environment expressed by a fitness value. When a new colour is created, its fitness is randomly drawn from some given distribution (we will experiment both with a uniform and a beta distribution). If the new colour has a fitness value higher than the average fitness in the population of existing coloured balls then the mutation is considered successful and **a new black ball** is also added. If instead the new colour has lower than average fitness, the mutation is considered unsuccessful and the number of black balls is kept unchanged.

To summarize, suppose that after $n - 1$ draws we have $n - 1$ coloured balls of k different colours and b black balls, then at time n :

- if a coloured ball is drawn it is re-introduced in the urn together with a new ball of the same colour, thus we will have n coloured balls of k different colours and b black balls;
- if a black ball is drawn a ball of a new colour is added to the urn and the new colour is assigned a random fitness f_{k+1} drawn from some given distribution:
 - if $f_{k+1} \geq \bar{f}$ (where \bar{f} is the average fitness) a new black ball is also added, thus we will have n coloured balls of $k + 1$ different colours and $b + 1$ black balls;
 - if $f_{k+1} < \bar{f}$ no further action is taken, thus we will have n coloured balls of $k + 1$ different colours and b black balls;

As to the calculation of \bar{f} , we use both a simple average over the colours without weighing them with the number of balls, or a weighted average in which every colour is attributed a weight consisting of the number of balls with that colour.

We have therefore two stochastic processes going on in parallel, one governing the number of black balls: $B_0 = 1$, $B_1 = 1$ or 2 , $B_2 = 1, 2$ or 3 and the other that we have already analyzed, determining the colour of the non-black ball added into the urn at time n : $X_1 = 1$, $X_2 = 1$ or 2 , $X_3 = 1, 2$ or 3 , where the probability of adding a new colour at time n is given by the number of black ball over the total number of balls, i.e. $B_{n-1}/(B_{n-1} + n - 1)$.

In the next sections we provide numerical results on the behaviour of this urn, starting however with two limit cases we will use as a benchmark.

3 Two benchmark cases

We first consider two limit cases. First, the case of a standard *Hoppe-Pólya* model, where there is only one black ball acting as mutator. Second, the opposite case in which one new black ball is added whenever a black ball has been drawn, irrespective of any fitness measure. We will refer to this second case as the *constant innovation* model.

In the case of a *Hoppe-Pólya model* innovation tends to disappear quickly, because the probability of extracting a black ball decreases in time as $\frac{1}{t}$. This is exemplified by looking at the time series of the number of colours in one simulation, as reported by the top panels of Fig. 3. A time series of the number of colours is an aggregate measure of the urn variety. At any time step we can look with more detail into the composition of the urn, by considering how the balls of different colours are distributed. In the bottom panels of Fig. 3 we report two analysis of balls counts at time $T = 7000$. In the bottom-left panel we plot the number of balls for each colour (mass vector), and in the bottom-right panel the allelic partition given by a frequency histogram. In this example we observe a relatively low variety, with two colours scoring more than one thousand balls, and in particular colour number two getting more than half the total population.

If we run the modified model with *constant innovation*, we obtain a completely different scenario. The results of a typical of simulation are reported in Fig. 4. The growth rate of the number of colours is slightly lower than linear, as the time series in the left panel suggests. Black balls (the mutator) follow the same dynamics of any other colour in this modified model. We know from Arthur et al. (1987) that in a pure *Polya model* a limit value for the relative fractions of colours exists, although this is not known *a priori*. This is not the case with the modification of the *constant innovation model*: whenever the black ball is selected, two balls are added (a new colour and another black), so in this case the increase in the total number of balls is twice as large as in the case in which a non-black ball is drawn. Overall, the total number of balls increases faster than t (but still slower than $2t$). As a consequence, the fraction of each colour

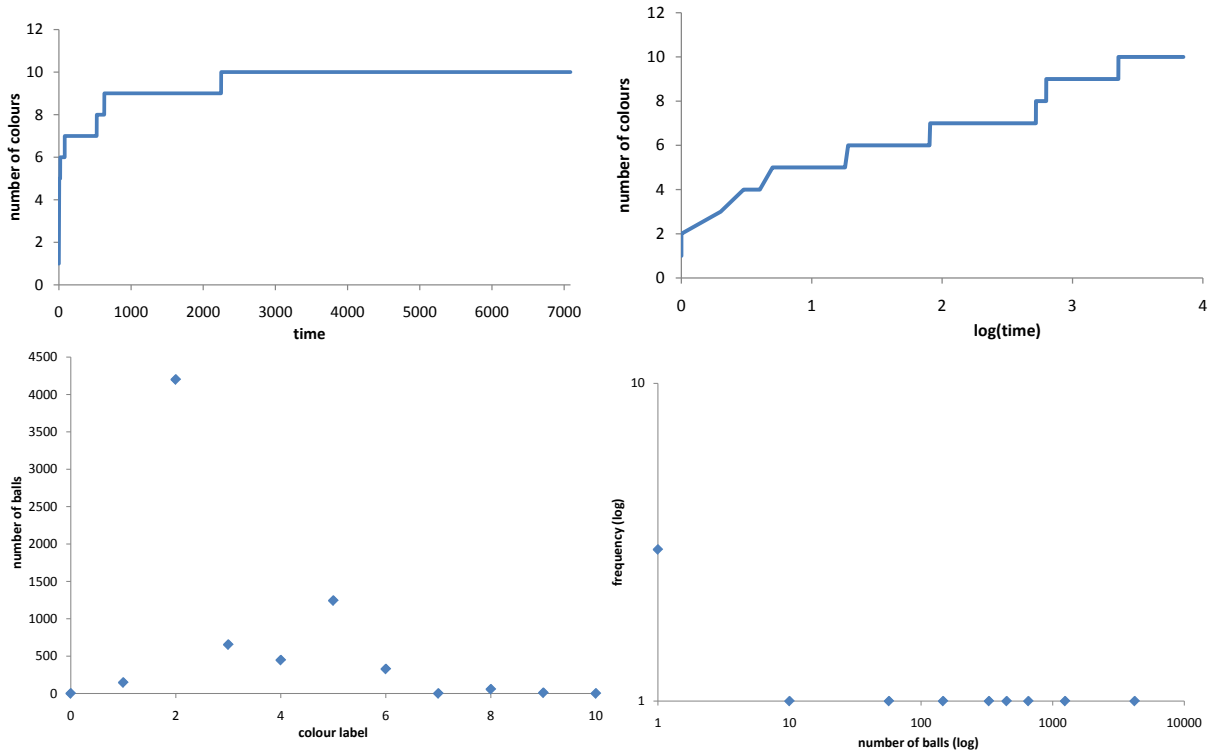


Figure 3: One simulation of the *Hoppe-Pólya* model. Top-Left: time series of the number of colours Top-Right: time series of the number of colours in logarithmic scale. Bottom-Left: colours mass vector (each colour is labeled with an integer number on the horizontal axis, while the vertical axis reports the number of balls of each colour). Bottom-Right: colours allelic partition in log-log scale (the vertical axis reports the frequency of a given number of balls).

does not converge to a positive limit value, but decreases steadily. Intuitively, this makes sense, because the system is expanding not only in size, but also in variety, and existing colours have to leave space for new colours. In particular, also the share of black balls decreases over time, and therefore the innovation rate decreases in the *constant innovation* model too, although more slowly than in the *Hoppe-Pólya* model.

Let us consider the colour mass vector (Fig. 4, bottom-left panel) and the colours frequency vector (bottom-right panel) of the urn at time $T = 5000$. If we compare with the case of the pure *Hoppe-Pólya* model, there are several colours with a substantial population, and the variety of the system is much larger. The frequency vector of colours in the bottom-right panel is approximately a straight line in a log-log scale, which indicates a power-law distribution for the allelic partition of the *constant innovation* model.

A more systematic way to compare the two models is obtained with a Monte Carlo approach, by running several simulations of the same model specification. Here we run experiments with 1000 repetitions on a time horizon of 2000 steps. Fig. 5 refers to the pure *Hoppe-Pólya* model, and reports the frequency histograms of the final number of colours (left panel) together with the entropy of the system (right panel).

Fig. 6 contains the results of an identical simulation experiment for the *constant innovation* model. We must keep in mind that in this limit case the black colour is no different from other colours, and the stochastic process of the number of black balls obeys exactly the same self-reinforcing dynamics. With respect to the pure *Hoppe-Pólya* model, we have by far many more colours. Moreover, the distributions of the number of colours are slightly skewed in opposite ways in the two cases. The most remarkable difference between the two specifications of the model is in the final entropy values. The model with *constant innovation* presents a very skewed distribution, while the distribution is fairly symmetric in the *Hoppe-Pólya* case. Secondly, the two distributions have approximately the same variance, but the tails of the two distributions

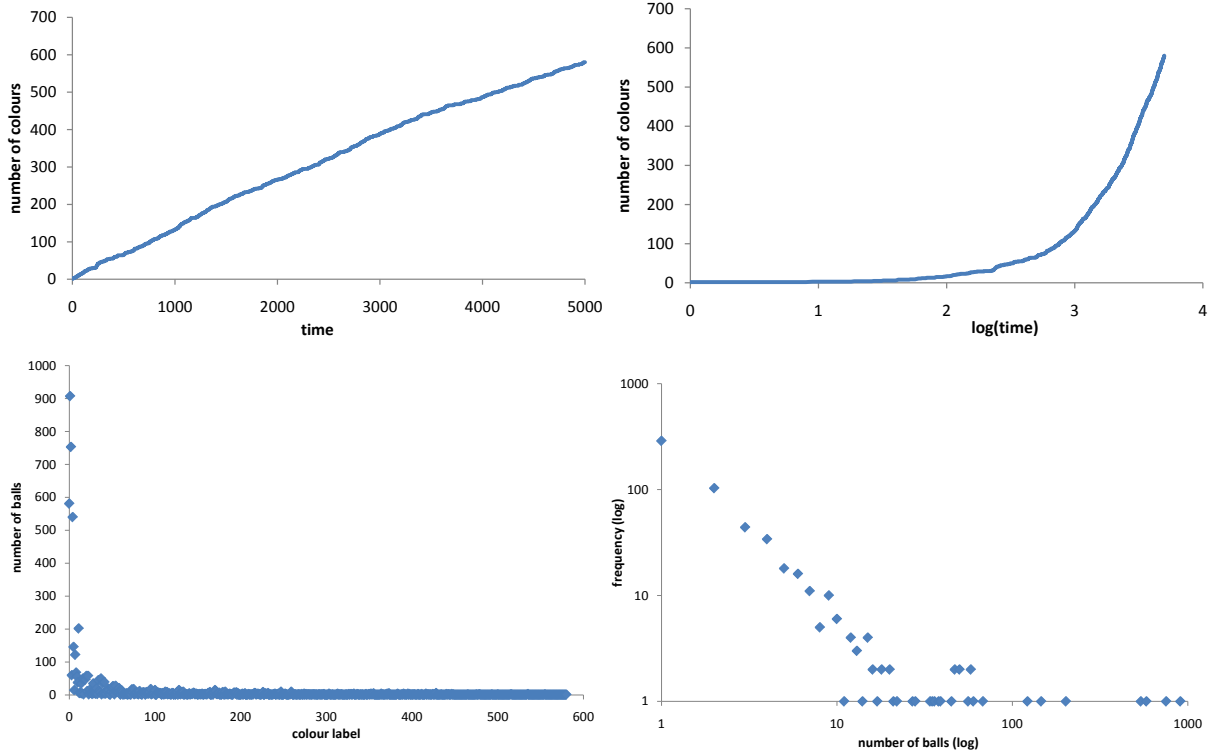


Figure 4: One simulation of the *constant innovation* model. Top-Left: time series of the number of colours Top-Right: time series of the number of colours in logarithmic scale. Bottom-Left: colours mass vector (each colour is labeled with an integer number on the horizontal axis, while the vertical axis reports the number of balls of each colour). Bottom-Right: colours allelic partition in log-log scale (the vertical axis reports the frequency of a given number of balls).

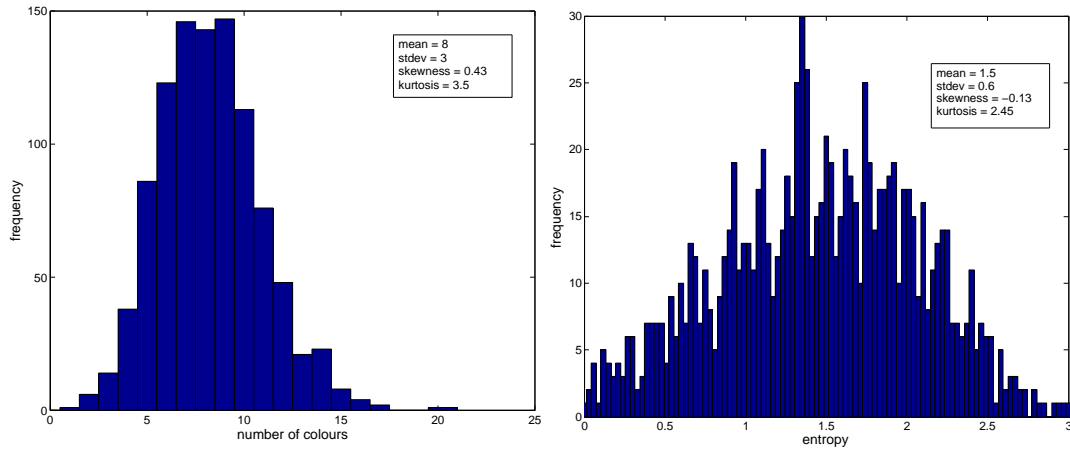


Figure 5: Batch simulations of the *Hoppe-Pólya* model. Distributions of 1000 runs after 2000 steps. Left: frequency histogram of the number of colours. Right: frequency histogram of the entropy.

are quite different. For the *Hoppe-Pólya model* the distribution of entropy values is relatively broad (platykurtic), while it is very peaked (leptokurtic) in the *constant innovation* model. Although the modification of the latter brings a much larger variety, as expected, the dispersion of outcomes is lower than in the *Hoppe-Pólya* model.

4 Adaptive urns

In the model with adaptive urns a newly drawn colour is assigned a fitness value from a uniform random distribution, $f_i \sim U[0, 1]$, and the mutator is “rewarded” with a new black ball only if

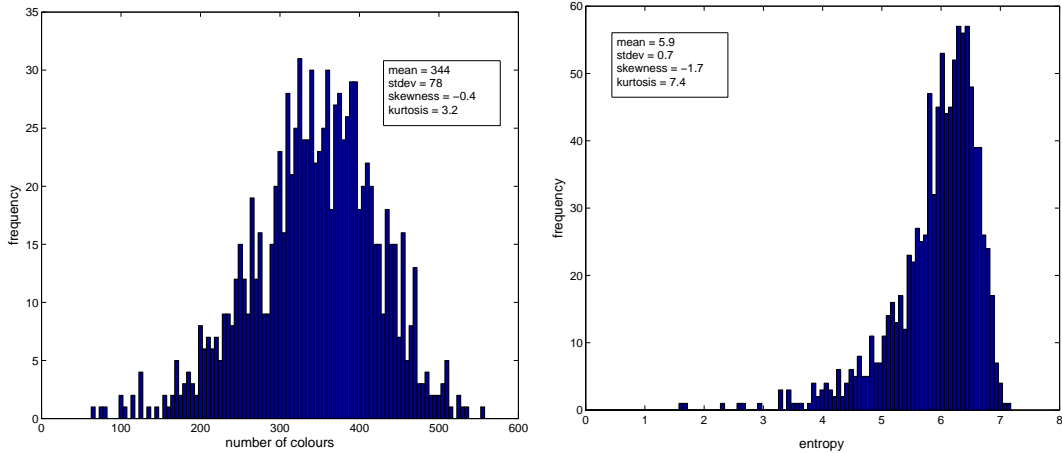


Figure 6: Batch simulations of the *constant innovation* model. Distributions of 1000 runs after 2000 steps. Left: frequency histogram of the number of colours. Right: frequency histogram of the entropy.

such fitness value is larger than the average fitness of balls in the urn, $f_i > \bar{f}$. Two specifications of the adaptive urns model are considered: one where we use the simple average of extracted fitness values across colour (i.e. if there exist k colours we average over k fitness values, without weighing for the number of balls of each colour), and an alternative one where the average fitness is weighted by the number of balls of each colour. We call these two versions of the model *Simple-average-fitness* and *Weighted-average-fitness*, respectively. Both specifications will be proposed in two versions of increasing complexity. In the first one the colours' fitness only acts on the self-reinforcing mechanism of the mutator, as specified above, while in a second version the fitness of a colour also enters the self-reinforcing mechanism through an allocation function which is not anymore the mere fraction of the balls of that colour in the population. In the final section we repeat the whole analysis of adaptive urns with a non-uniform distribution of fitness values, namely the Beta distribution.

Let us begin with the *Simple-average-fitness* model. This model is appropriate if one thinks of balls as technologies or products or species. Fig. 7 reports the results of one simulation run lasting for $T = 2000$ steps. First of all, the number of colours increases faster than in the *Hoppe-Pólya* model, but slower than in the *constant innovation* model (top panels). Moreover, we notice that periods without innovation are followed by periods of relatively frequent innovations that cluster in time. The explanation of this behaviour is as follows. Innovations alter the average fitness, which is the reference point for an innovation to be considered as 'successful'. A successful innovation raises this reference point, while unsuccessful innovations do the opposite. On top of this, the main factor driving the dynamics of the average fitness is the self-reinforcing process of ball extraction, which is proportional to the frequency of colours. If a colour with relatively low fitness happens to become dominant, the probability of successful innovation goes up. If instead a colour with relatively high fitness becomes dominant, innovation becomes more and more difficult. In the first case, successive waves of innovation may occur, while in the second case the dynamics presents long periods without innovation.

The middle panels of Fig. 7 contain the colour vector (left) and the allelic partition (right) at time $T = 2000$. We observe a richer scenario than in the pure *Hoppe-Pólya* model, with a number of different colours being characterized by more than one ball, but still much less variety than in the *constant innovation* model. The frequency distribution of the number of balls of each colour (middle-right panel), the allelic partition of the urn, is still linear in log-log scale, but it presents a smaller value of the intercept with the horizontal axis with respect to the *constant*

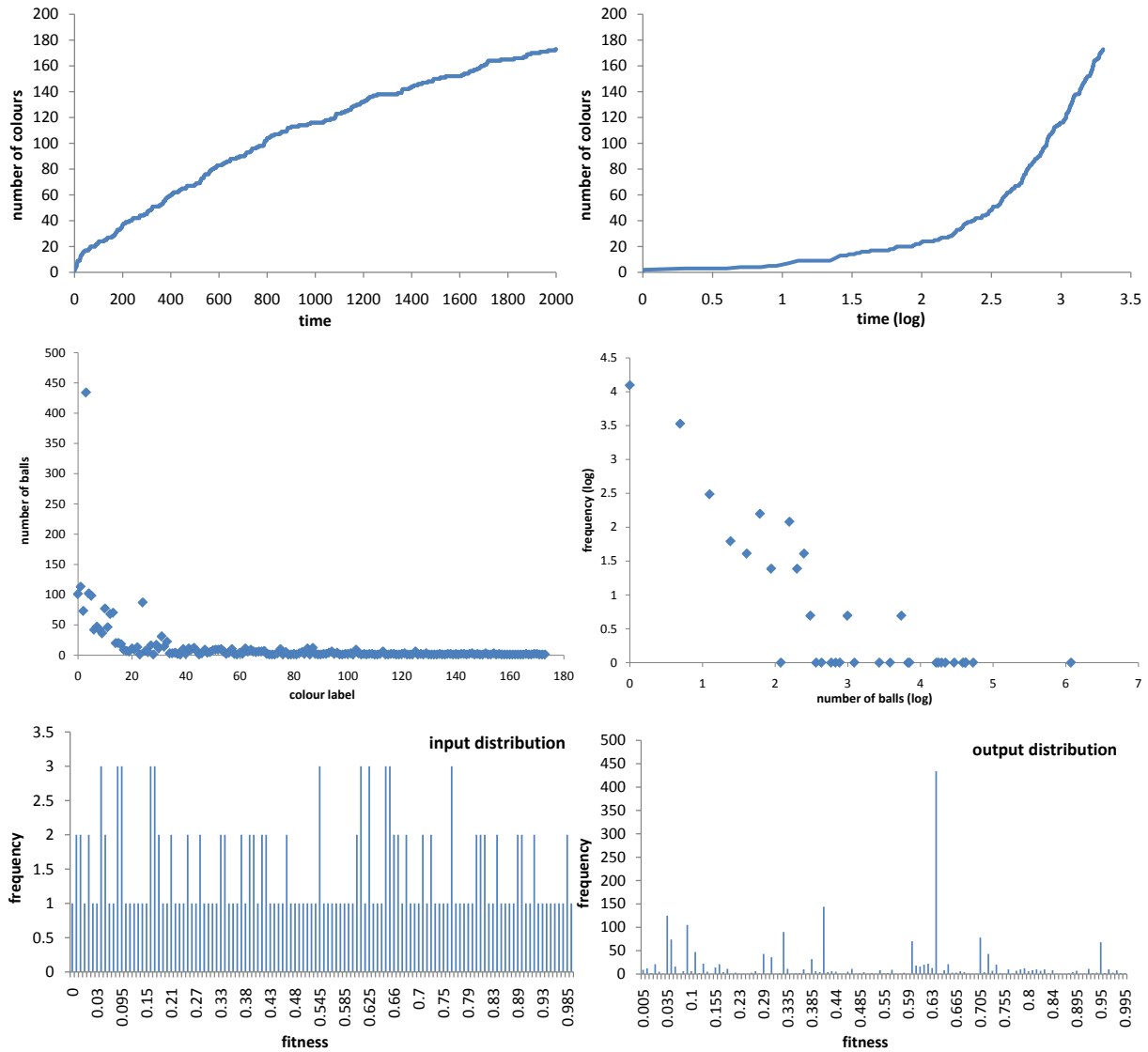


Figure 7: One simulation of the *Simple-average-fitness* model. Top-Left: time series of the number of colours. Top-Right: time series of the number of colours in logarithmic scale. Middle-Left: colours mass vector (each colour is labeled with an integer number on the horizontal axis, while the vertical axis reports the number of balls of each colour). Middle-Right: colours allelic partition in log-log scale (the vertical axis reports the frequency of a given number of balls). Bottom-Left: input fitness distribution (Uniform). Bottom-Right: output fitness distribution

innovation model.⁴

The bottom panels of Fig. 7 report the ‘input’, or initial, fitness distribution (bottom-left panel), and the ‘output’, or final, fitness distribution of balls. The input values are a realization of the input distribution of new balls. The output is how balls’ fitness values are distributed at time $t = 2000$. This distribution is not uniform anymore: the model ‘selects’ a small numbers of fitness values as a result of the Polya scheme self-reinforcing process.

In Fig. 8 we report the results for one simulation run of the model in the *Weighted-average-fitness* specification. If we are to compare the results of simulations in Figures 7 and 8, their qualitative behaviour is quite similar. The former ends with a larger number of colours, as testified by the time series in the top panels and with the allelic partition in the middle-right panels. Such slightly different outcome is not due to the different specifications of the model

⁴Notice that simulations with the same time horizon and the same number of innovations may have a different final number of balls, because successful innovation events add two balls instead of one.

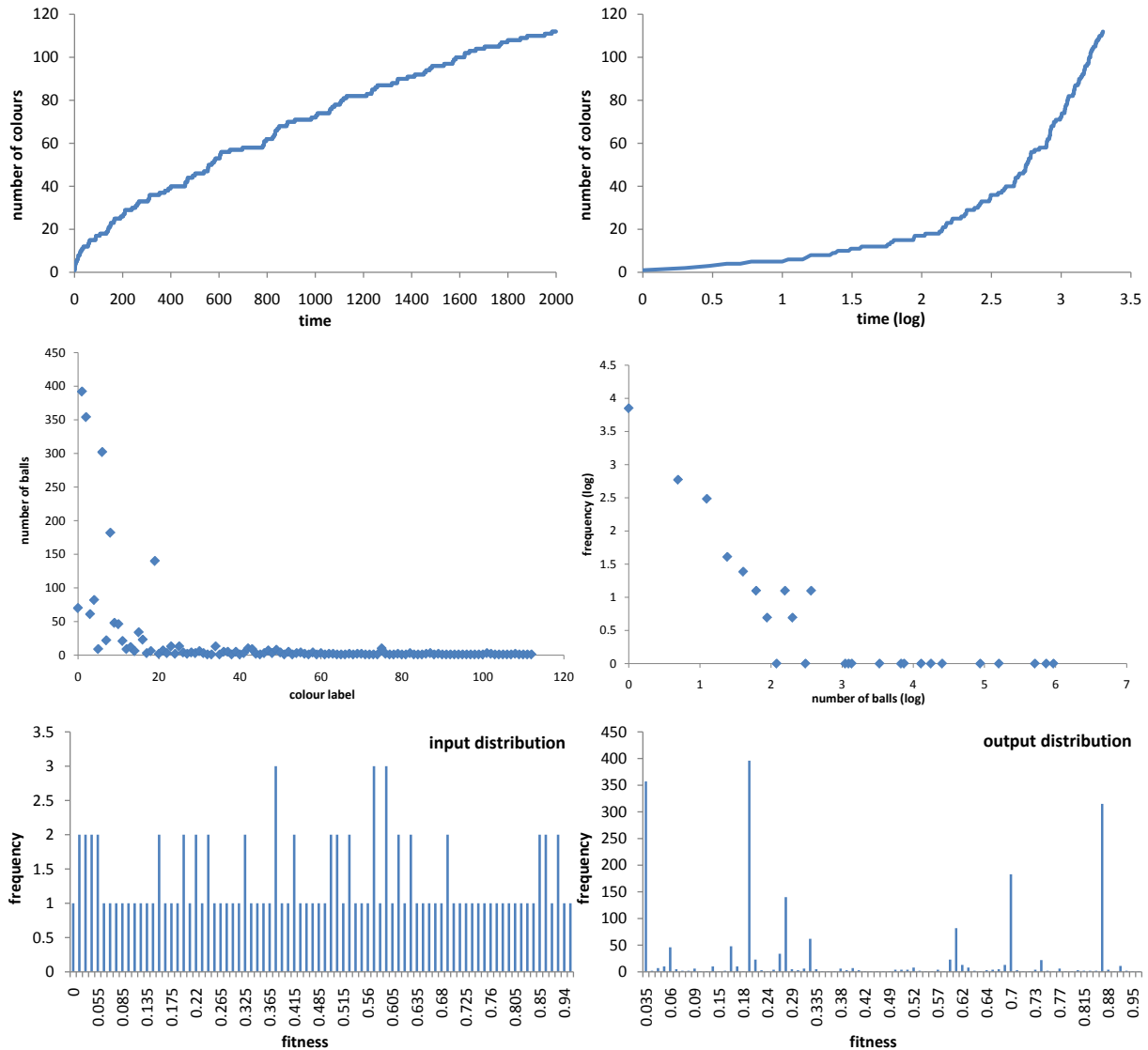


Figure 8: One simulation of the *Weighted-average-fitness* model. Top-Left: time series of the number of colours Top-Right: time series of the number of colours in logarithmic scale. Middle-Left: colours mass vector (each colour is labeled with an integer number on the horizontal axis, while the vertical axis reports the number of balls of each colour). Middle-Right: colours allelic partition in log-log scale (the vertical axis reports the frequency of a given number of balls). Bottom-Left: input fitness distribution (Uniform). Bottom-Right: output fitness distribution

but to the path-dependent dynamics of the process, heavily influenced by early events of black ball extraction. We have noticed that simulations of the *Simple-average-fitness* model are more stable, while the *Weighted-average-fitness* model presents a larger variability in terms of the final number of balls and their distribution of fitness values. This is due to the sharper measure of average fitness of the *Simple-average-fitness* model, as we will see next with batch simulation experiments.

Two aspects must be stressed here about path dependence in the model. The first has to do with the self-reinforcing dynamics of Markov chains driving the competition of alternative options, which obeys to the probabilistic rules studied extensively by Arthur et al. (1987). In this model, as in ours, there is a limit value of the relative frequencies, but this limit is not known *a priori*. What makes the difference in our model is that competing options are not given and fixed, but increase in number due to innovation. Also innovation is path-dependent, as in the constant innovation benchmark case, and its pace depends on its own realizations. But in our model innovation is also “adaptive”, since it also depends on the average fitness of species.

This dependence has the connotation of a negative feedback: whenever high fitness variants are created, the number of black balls tends to increase fast. But this ‘prepares’ the ground for low innovation rates in following steps, because the average fitness goes up and successful innovation becomes less likely.

We now turn to batch simulation experiments for both specifications of the adaptive urns model. Beside the *number-of-colours*, we now also look at the *simple-average-fitness* and the *weighted-average-fitness* of the urn. These measures represent the reference value a ‘successful’ innovation in the two different specifications of the model. Let us start with the *simple-average-fitness* model. Fig. 9 reports the distribution of simulation outcomes at the end of a time horizon $T = 2000$ time steps. The results are remarkably different with respect to the model

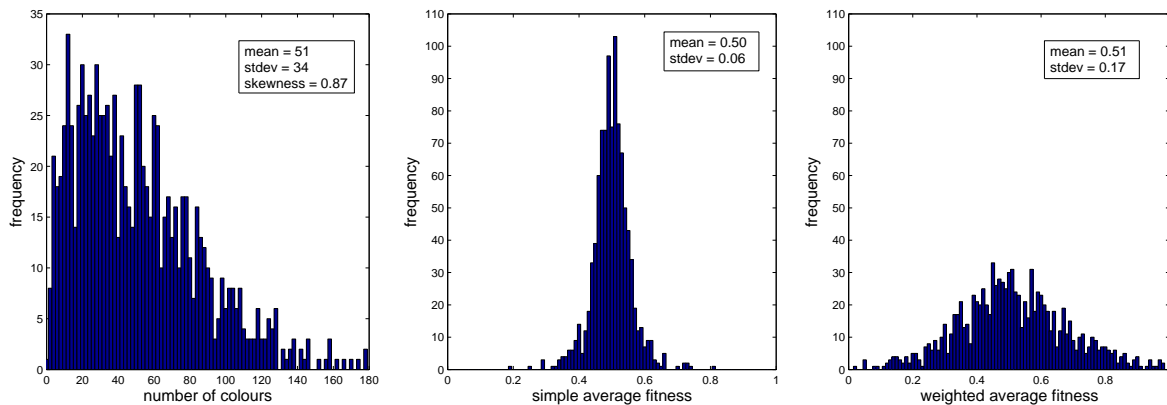


Figure 9: Batch simulations (1000 runs) of the model *Simple-average-fitness* with time horizon $T = 2000$ steps. Left: frequency histogram of the number of colours. Centre: frequency histogram of the average fitness of colours. Right: frequency histogram of the weighted average fitness of colours.

without fitness values. The distribution of the number of colours (left panel) is highly skewed: most simulations end with a small number of colours. These results should be compared to Fig. 5 (*Hoppe-Pólya* model) and Fig. 6 (*constant innovation* model). As expected, a selection mechanism based on fitness lowers the number of colours with respect to the *constant innovation* model. If the first colours introduced in the early stages of the simulation are ‘unsuccessful’,

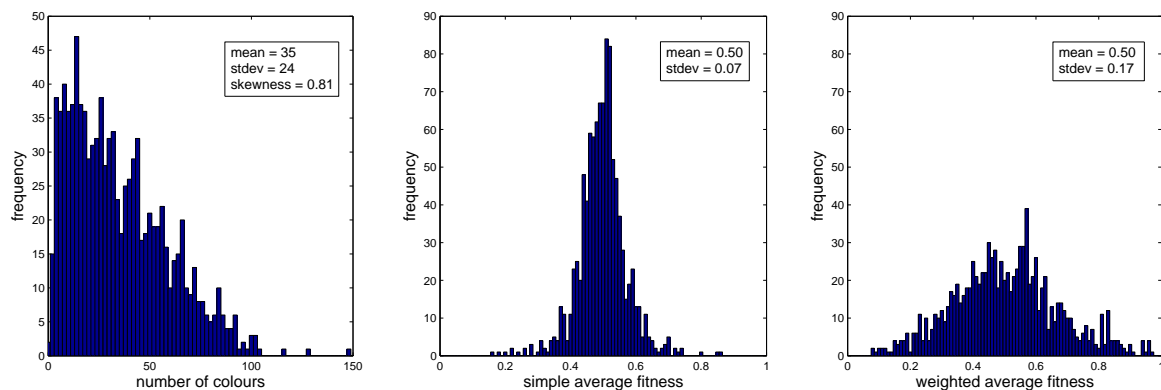


Figure 10: Batch simulations (1000 runs) of the model *Simple-average-fitness* with time horizon $T = 1000$ steps. Left: frequency histogram of the number of colours. Centre: frequency histogram of the average fitness of colours. Right: frequency histogram of the weighted average fitness of colours.

the fraction of black balls goes down relatively rapidly, and with this the urn innovation rate, which leads to low variety for the rest of urn process. Fig. 10 reports the outcomes for a batch simulation of the same model after a shorter time horizon, $T = 1000$. The distribution

of simple and weighted average fitness for the two different time horizons are almost identical, which indicates a stable probability distribution for the stochastic process of the model.

The simple average fitness distribution is very concentrated around the fitness mean value $1/2$ (Fig. 9, central panel), while the distribution of the weighted average fitness is much broader (right panel). Both features can be empirically relevant, with the *Simple-average-fitness* model pointing to systems with relatively low variety, and the *weighted-average-fitness* being more appropriate for scenarios with higher uncertainty.

The batch simulations results for the *Weighted-average-fitness* model are reported in Fig. 11. The final distributions of simple and weighted average fitness in the two models are very similar.

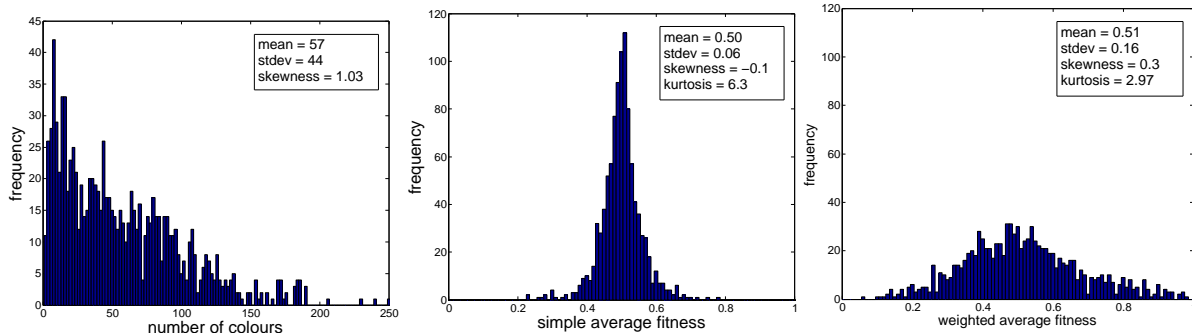


Figure 11: Batch simulations (1000 runs) of the *weighted-average-fitness* model with time horizon $T = 2000$ steps. Top-left: frequency histogram of the number of colours. Top-right: frequency histogram of the entropy. Bottom-left: frequency histogram of the simple average fitness of colours. Bottom-right: frequency histogram of the weighted average fitness of colours.

What is quite different is the distribution of the final number of colours. The *simple-average-fitness* presents a lower dispersion of outcomes, expressed by a lower mean, a lower standard deviation and also a less skewed distribution (Fig. exp20130416b, left panel), if compared to the *weighted-average-fitness* model. The reason behind this outcome is the following. The lower dispersion of the simple average fitness measure (central panels of Figures 9, 10 and 11) makes this one a sharper reference point for the definition of ‘successful’ innovations, $fitness(innovation) > average-fitness$. Consequently, we can expect a lower dispersion of innovation rates across different simulation runs for the model based on this type of average measure. This translates into less variety for the *simple-average-fitness* model, as presented by the distribution of the final number of colours: for instance, the highest number of colours obtained with the simulation experiment reported in Fig. 9 (*simple-average-fitness* model) is 180, against 250 colours in the experiment of Fig. 11 (*weighted-average-fitness*).

5 Non-uniform distribution of colours fitness

In this section we study the adaptive urn model with a non-uniform distribution of fitness values. We use a Beta distribution of fitness values, for which the probability density function reads as follows:

$$\Phi(f; \alpha, \beta) = \frac{1}{B(\alpha, \beta)} f^{\alpha-1} (1-f)^{\beta-1}, \quad f \in [0, 1]. \quad (4)$$

The factor $\frac{1}{B(\alpha, \beta)}$ is a constant, defined by $B(\alpha, \beta) = \int_0^1 t^{\alpha-1} (1-t)^{\beta-1}$. The parameters α and β control the probability distribution, whose density function can be increasing, decreasing or non monotonic. Accordingly, the cumulative distribution function $\Phi(f)$ can be convex, concave or S-shaped. The uniform distribution is a special case obtained with $(\alpha = 1, \beta = 1)$. We consider the following cases: $(\alpha = 1, \beta = 3)$, $(\alpha = 2, \beta = 2)$, $(\alpha = 3, \beta = 2)$, $(\alpha = 3, \beta = 1)$ (Figure 12). The mean values are given by $\alpha/(\alpha + \beta)$, and are $1/4$, $1/2$, $3/5$ and $3/4$, respectively.

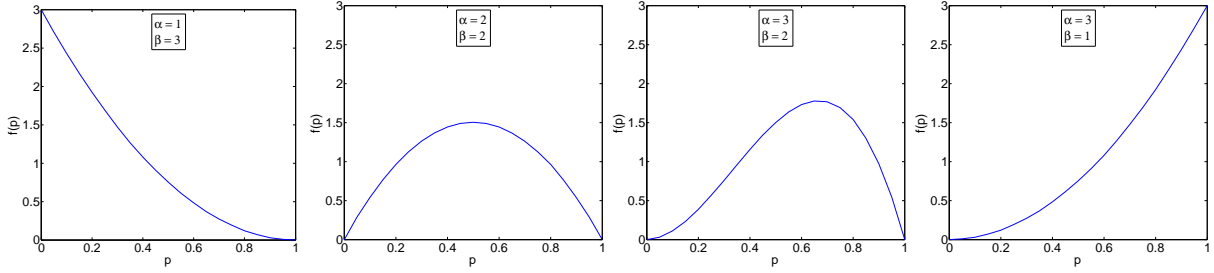


Figure 12: Beta distribution density function, four cases.

We study the model with a Monte Carlo approach, as before. In each condition, we run 1000 simulation runs for 2000 periods, and look at the final distributions of *number of colours*, *simple average fitness*, *weighted average fitness* and *entropy*. In the case of the model that uses the simple average fitness as a reference value for a successful innovation, the *Simple-average-fitness* model, we obtain the results reported in Figure 13. We observe the following. First, whenever

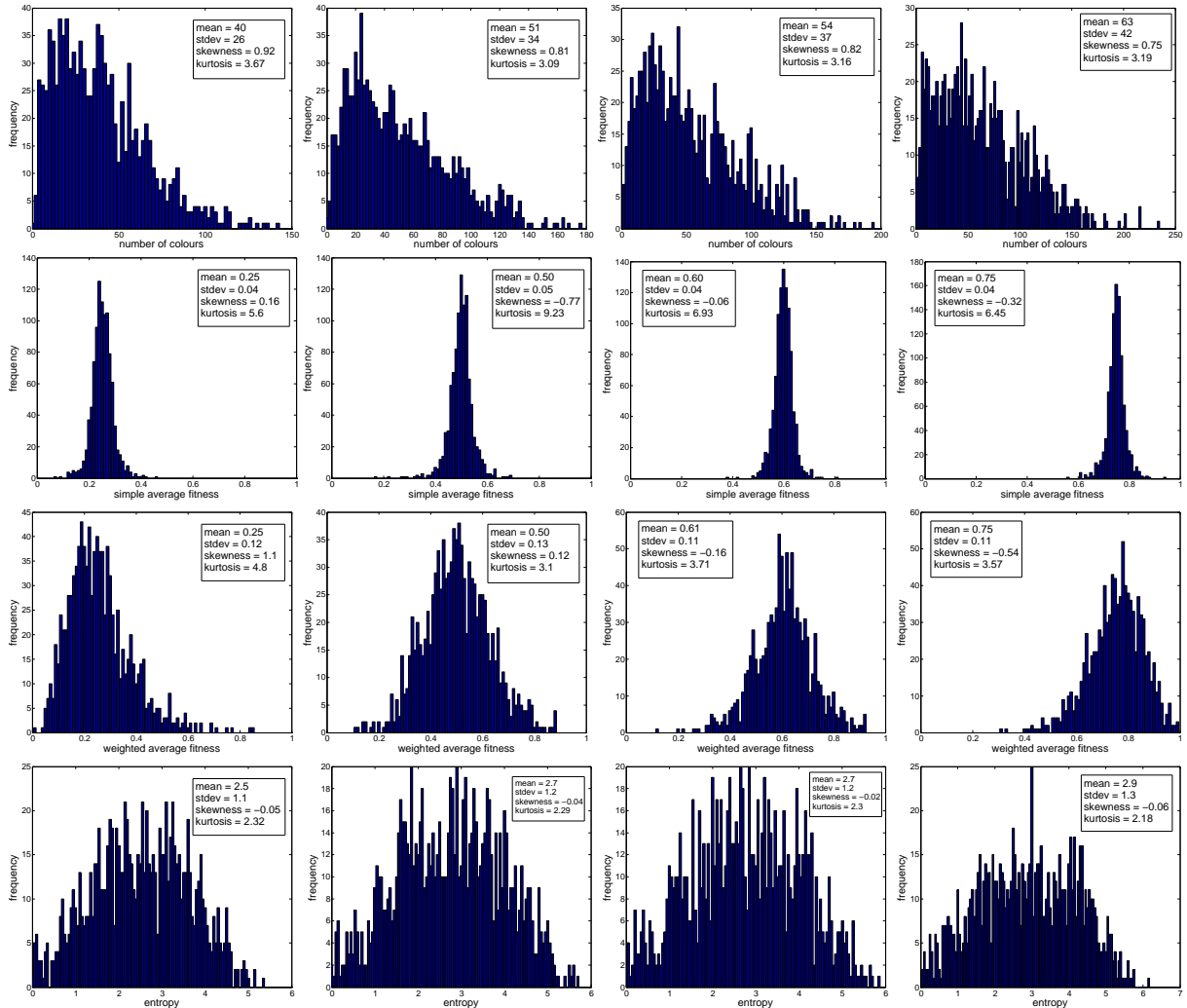


Figure 13: *Simple-average-fitness* model with non-uniform fitness values: Left: $Beta(1, 3)$. Centre-Left: $Beta(2, 2)$. Centre-Right: $Beta(3, 2)$. Right: $Beta(3, 1)$. Histograms report the distributions of the *number of colours*, *simple average fitness*, *weighted average fitness* and *entropy*, after $t = 2000$ periods for 1000 simulation runs.

the initial distribution of fitness values has more probability mass on larger values, we obtain, on average, a larger number of colours in the urn at any given time, with a larger dispersion of

outcomes (Fig. 13, top panels). The distribution remains positively skewed, though. Second, the probability mass of the initial fitness values drives the location of the final distribution both of simple and of weighted average fitness values: for example, with an initial probability distribution $Beta(1, 3)$, we have a mean average fitness equal to 0.25 ± 0.04 , with $Beta(2, 2)$ we get 0.50 ± 0.05 , with $Beta(3, 2)$ we get 0.60 ± 0.04 while with $Beta(3, 1)$ we obtain a mean at 0.75 ± 0.04 . The same mean values are obtained in terms of weighted average fitness, but with much larger variance (almost thrice as much). It is important to notice how the mean values are exactly the theoretical mean values of the starting fitness distribution.

A third observation is about the shape of the weighted average fitness distribution. While a uniform starting distribution of fitness values gives a nearly Gaussian distribution, non-uniform distributions make the final outcomes deviate both in terms of skewness and kurtosis. Except for the $Beta(2, 2)$ starting distribution, which is symmetric, the other three give a leptokurtic distribution of final weighted average fitness values. Moreover, a non-symmetric probability mass makes the final distribution skewed, either positively, or negatively, depending on whether the mode of the starting distribution is below or above the mean.

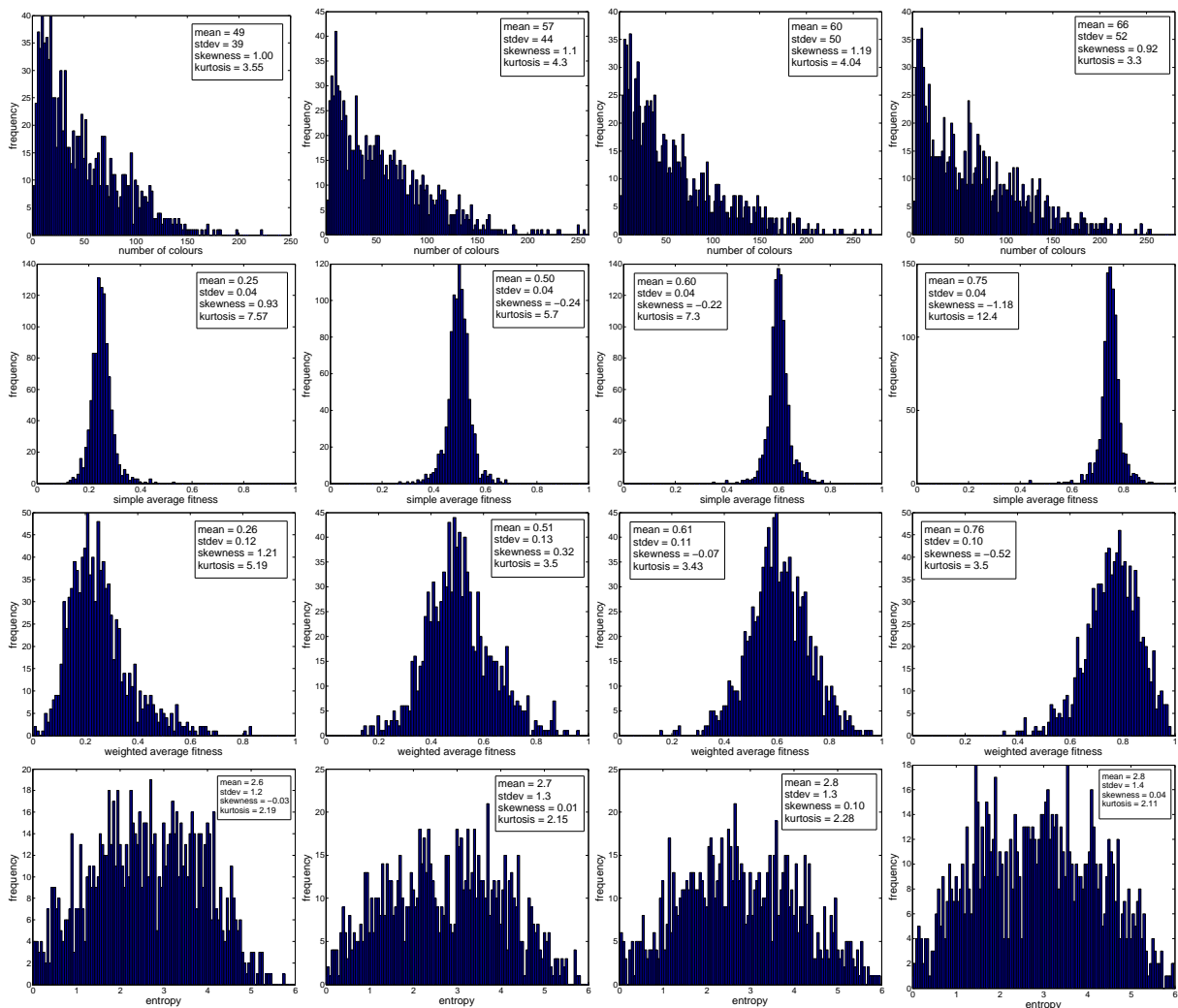


Figure 14: *Weighted-average-fitness* model with non-uniform fitness values: Left: $Beta(1, 3)$. Centre-Left: $Beta(2, 2)$. Centre-Right: $Beta(3, 2)$. Right: $Beta(3, 1)$. Histograms report the distributions of the *number of colours*, *simple average fitness*, *weighted average fitness* and *entropy*, after $t = 2000$ periods for 1000 simulation runs.

The final observation concerns variety, as expressed by the final entropy distribution. Although outcomes are quite similar across the different starting distributions, we observe a slight increase in the mean entropy as we put more probability mass on larger initial values, from 2.5

up to 2.9. This means that a starting fitness probability distribution with more weight on larger values leads to larger variety in the urn.

In Figure 14 we report the batch simulations results for the *Weighted-average-fitness* model. By comparing these results with the results for the *Simple-average-fitness* model in Figure 13 we see some differences in the distributions of the final number of colours. The *Weighted-average-fitness* model produces a larger number of colours on average (top panels in Fig. 14) for all four initial Beta distributions. Similarly, also the variance is larger. This leads to distributions of the final number of colours in the urn that are more skewed in the *Weighted-average-fitness* model than in the *Simple-average-fitness* model, a feature that we observe also with a uniform distribution of starting fitness values (Figures 9 and 10). Regarding the distributions of simple and weighted average fitness, and entropy, the two models give very similar results.

Our model can describe the birth and growth processes subject to innovation and positive feedback and such as cities or firms. In this interpretation fitness can represent a size measure, with many colours of small size and few colours of large size. In order to build on this interpretation of the model, a statistical characterization of the number of colours distribution is needed. For instance, if one looks at the size distribution of cities, the model's parameters should be set in order to obtain the empirical Zipf law distribution (Gabaix, 1999). Alternatively, the adaptive urn model can be used to explain the statistical features of firms' growth rates (Bottazzi and Secchi, 2006). In any case, the initial distribution of fitness values is one factor where parameters can be set in order to match the empirical distribution of interest with the model. A second factor is the choice between the weighted and the simple average fitness specification of the model for the reference value of successful innovation: if more variability is needed, the *weighted-average-fitness* model is more appropriate, while for relatively lower variability scenarios the best choice is the *simple-average-fitness* model. In the next section we introduce a further factor that increases the flexibility of the model in view of its empirical calibration: a selection of colours based not only on the self-reinforcing mechanism of their relative share, but also based on the measure of fitness.

6 Fitness-based selection of colours

In this section we present the final extension of our urn scheme model with innovation, where not only the probability of introduction of new colours but also the probability of enforcement of the existing colours is dependent upon fitness values.

In the previous versions of the model any colour has a probability of extraction equal to the fraction of balls of that colour in the urn, while its fitness only serves to reward the urn innovation factor by comparing it to the balls' average (simple or weighted) fitness. We now bring the fitness into the colours' extraction mechanism. For each colour i already present in the urn, we define its extraction probability as follows:

$$\pi_t^i = \frac{x_t f^i}{\sum_{j=1}^{n_t} x_t^j f^j}, \quad (5)$$

where x_t is the colour fraction at time t , f^i its fitness, and n_t the number of colours at time t .

Let us first compare the *simple-average-fitness* and *weighted-average-fitness* specifications of the model equipped with the new probability of colour extraction as given by Eq. (5). Figure 15 reports batch simulations which, apart from this new probability of ball addition, use the same settings as the previous sections. In both model specifications we obtain a much larger number of colours if compared to the models discussed in the previous section. The distribution of the final number of colours is not decreasing anymore as it is in Figures 9 and 11 and presents a peak at a relatively large number of colours, between 600 and 700. In the *simple-average-fitness* model (left panel of Fig. 15) the distribution is unimodal, with about 660 colours being the

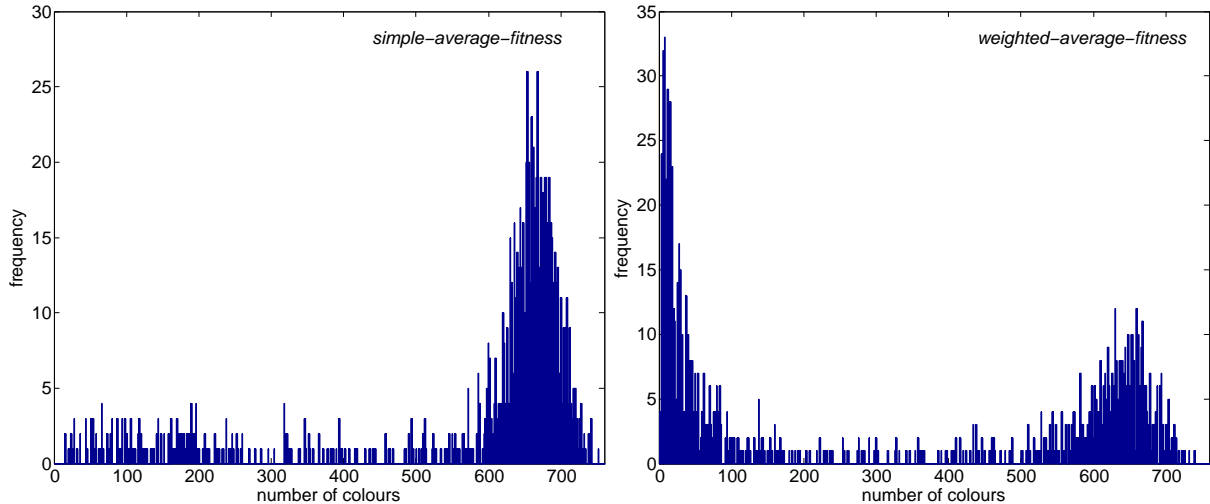


Figure 15: Adaptive urn model with fitness-based selection of colours. Left: *simple-average-fitness* model. Right: *weighted-average-fitness* model. Histograms collect 1000 simulation runs. Each run lasts for $T = 2000$ periods.

most frequent outcome. This is not the case for the *weighted-average-fitness* model, that gives a bi-modal distribution. In this case, a relatively large number of simulations end up with few colours, and the second peak is less pronounced. The mode is also slightly smaller with a number of colours around 650 being the most frequent one. In the *weighted-average-fitness* model there is a threshold effect in the colour generation mechanism of the adaptive urn process. Innovation (the black ball) is rewarded if the fitness of new colours is above the weighted average. But if such new colours become too abundant, the weighted average increases, the innovation rate goes down and the number of different colours increases more slowly. This effect is absent in the *simple-average-fitness* model, where the relative weight of colours does not count in the innovation reinforcement mechanism. In this case the fitness dependent selection mechanism (equation 5) boosts the diversity of the system, while in the *weighted-average-fitness* model this occurs only partially, because the increasing share of high fitness balls makes successful innovation less and less likely.

Finally, we introduce a parameter γ that controls the relative strength of fraction and fitness factors, and re-define the colours extraction probability as

$$\pi_t^i = \frac{(x_t^i)^\gamma (f^i)^{(1-\gamma)}}{\sum_{j=1}^{n_t} (x_t^j)^\gamma (f^j)^{(1-\gamma)}}. \quad (6)$$

This definition has two useful features. First, it includes the previous versions of the model of Sections 4 and 5, which is given obtained with setting $\gamma = 1$ (while with $\gamma = 0$ the extraction probability is proportional to the colour fitness). Second, the new parameter allows to calibrate the model on empirical data, and makes it prone to applications in different domains and scenarios.

We analyse this last specification of the fitness-based adaptive urn model by focusing on the *simple-average-fitness* version. Figure 16 reports batch simulation results in terms of the final number of colours (left panels) together with the final entropy of the urn (right panels). When γ is low, the fitness value is preponderant in the colours extraction probability (6). This condition produces a relatively larger number of colours on average, with relatively less dispersion (top-left panel of Figure 16). A low γ , on the contrary, puts more weight on the colours fraction than on their fitness, which results in a lower number of colours on average, with more dispersion (bottom-left panel of Figure 16). Increasing γ we take the model closer to the specification of previous sections, where the colours extraction probability is only given by their relative share. In terms of entropy, we notice no differences for what concerns the mode of the distribution

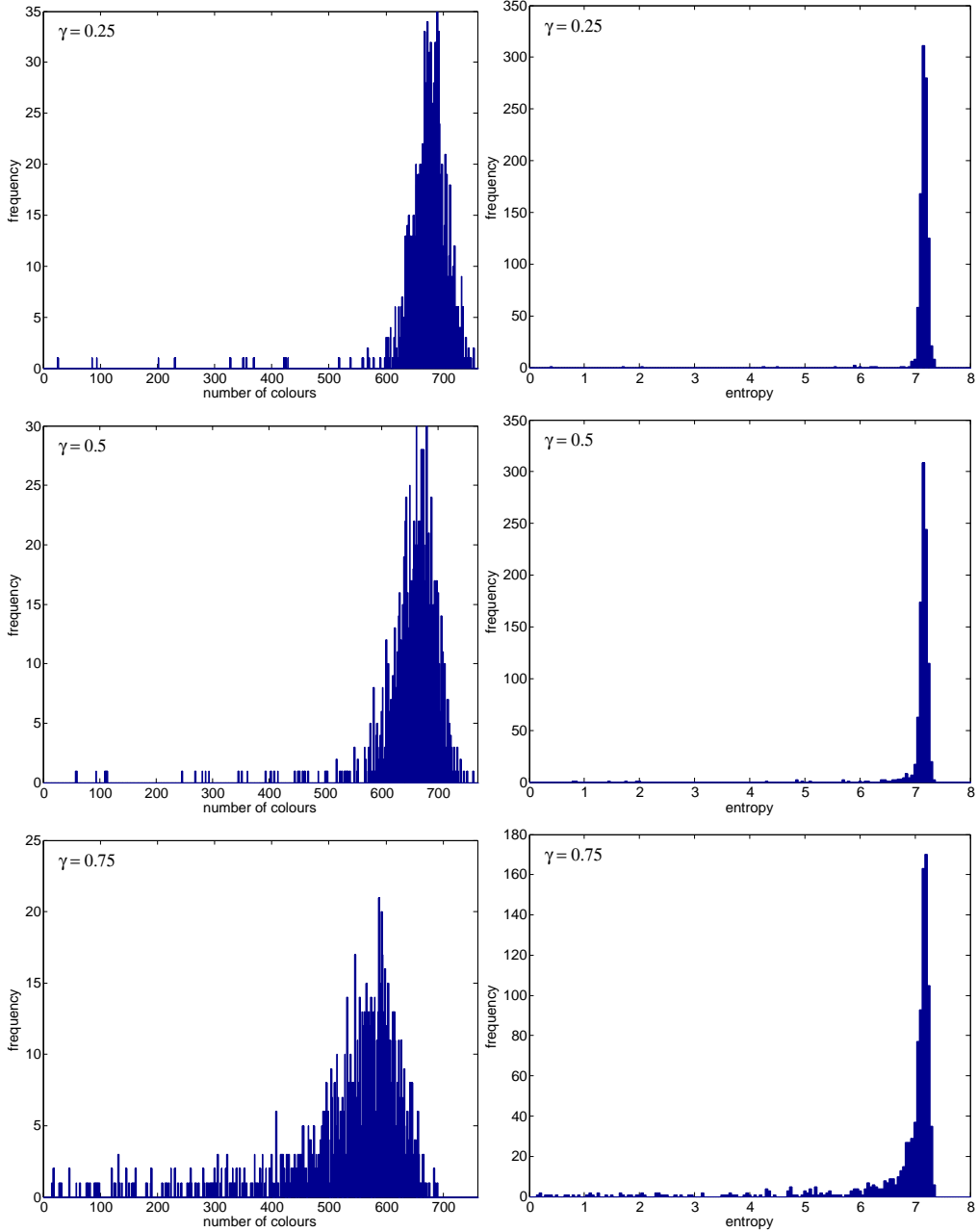


Figure 16: *Simple-average-fitness* model with the second specification of fitness-based selection of colours (Eq. 6). The parameter γ weights the contribution of fitness to the colours extraction probability. Left: final number of colours. Right: final entropy. Histograms collect 1000 simulation runs. Each run lasts for $T = 2000$ periods.

between $\gamma = 0.25$, $\gamma = 0.5$ and $\gamma = 0.75$, which is slightly above 7 in all three cases. A larger γ only marginally increases the dispersion of results, with few simulations ending with a substantially lower entropy.

Concluding, the specification of Eq. (6) enables to tune the model by giving more or less importance to the fraction or the fitness of colours by setting the parameter γ . This feature makes the model better equipped for applications to real cases of stochastic growth, making it possible a calibration of empirical data. Examples are the birth and growth process of cities, and the growth rate of firms.

7 Conclusions

The phenomenon of path dependence has attracted the attention of many scholars interested in the evolution of technologies (David, 1985; Arthur, 1989) or of social, economic and political institutions (David, 1985; Pierson, 2000). However, the conclusions supporting path dependence and lock-in and coming both from empirical evidence and from analytical models have also been questioned and criticized (Liebowitz and Margolis, 1995). But, while the criticisms of Liebowitz and Margolis are raised from a neoclassical perspective on the grounds of the belief that inefficient allocations cannot be persistent and will be always remedied by the market, in this paper we have on the contrary attempted to provide some tools that could extend the standard models of path dependence on the grounds a more comprehensive evolutionary perspective.

Standard models based on Pólya urns only consider a selection process among given alternatives and do not allow for the arrival of novelty and variation. In this paper we have introduced some extensions of urn models in which, in addition to the stochastic process governing selection, there exists another stochastic process for novelty generation. Paraphrasing Liebowitz and Margolis, we could say that lock-in into a supposedly inferior technology like VHS (as opposed to Betamax) is ultimately itself going to be transient not so much because market efficiency will take its revenge but because both VHS and Betamax may finally be displaced by the arrival of the DVD technology. The models we simulated in this paper can account for this complex interplay between selection among the alternatives available in some given time span and the arrival of new alternatives which changes the domain on which selection operates.

In this paper we have analyzed by means of numerical simulations the properties of different specifications of urn models with stochastic additions of new colours. We believe that these models can be calibrated in such a way as to give us useful insight on real cases of evolution of technologies, organizations and institutions whereby phases in which path dependent selection among given alternative are followed by phases in which the dynamics is mainly driven by the introduction of new alternatives. But the exploration of these empirical applications is left for future work.

References

- ALEXANDER, J. M., B. SKYRMS, AND S. ZABELL (2012): “Inventing new signals,” *Dynamic Games and Applications*, 2, 129–145.
- ARTHUR, B. (1989): “Competing technologies, increasing returns, and lock-in by historical events,” *Economic Journal*, 99, 116–131.
- ARTHUR, W., Y. ERMOLIEV, AND Y. KANIOVSKI (1987): “Path-dependent processes and the emergence of macrostructure,” *European Journal of Operation Research*, 30, 294–303.
- BOTTAZZI, G. AND A. SECCHI (2006): “Explaining the distribution of firms growth rates,” *RAND Journal of Economics*, 37, 235–256.
- CRAWFORD, V. AND J. SOBEL (1982): “Strategic Information Transmission,” *Econometrica*, 50, 1431–1451.
- DAVID, P. (1985): “Clio and the economics of QWERTY,” *American Economic Review*, 75, 332–337.
- DOSI, G., Y. ERMOLIEV, AND Y. KANIOVSKI (1994): “Generalized urn schemes and technological dynamics,” *Journal of Mathematical Economics*, 23, 1–19.

- EREV, I. AND A. ROTH (1998): "Predicting how people play games: reinforcement learning in experimental games with unique, mixed-strategy equilibria," *American Economic Review*, 88, 848–881.
- EWENS, W. J. (1972): "The sampling theory of selectively neutral alleles," *Theoretical Population Biology*, 3, 87–112.
- GABAIX, X. (1999): "Zipf's law and the growth of cities," *American Economic Review*, 89, 129–132.
- HOPPE, F. (1984): "Polya-like urns and the Ewens' sampling formula," *Journal of Mathematical Biology*, 20, 91–94.
- LIEBOWITZ, S. AND S. MARGOLIS (1995): "Path Dependence, Lock-in and History," *Journal of Law, Economics and Organization*, 11, 205–226.
- PIERSON, P. (2000): "Increasing Returns, Path Dependence, and the Study of Politics," *American Political Science Review*, 92, 251–267.
- PITMAN, J. (2006): *Combinatorial Stochastic Processes*, Berlin: Springer-Verlag.
- ZABELL, S. L. (1992): "Predicting the unpredictable," *Synthese*, 90, 205–232.